Chameleon-like Self-Assembling Peptides for Adaptable Biorecognition Nanohybrids

Woo-jin Jeong, Sung-ju Choi, Jun Shik Choi, and Yong-beom Lim*

Translational Research Center for Protein Function Control and Department of Materials Science & Engineering, Yonsei University, 50 Yonsei-ro, Seodaemun-gu, Seoul 120-749, Korea

ABSTRACT We present here the development of adaptable hybrid materials in which self-assembling peptides can sense the diameter/curvature of carbon nanotubes and then adjust their overall structures from disordered states to α-helices, and *vice versa*. The peptides within the hybrid materials show exceptionally high thermal-induced conformational stability and molecular recognition capability for target RNA. This study shows that the context-dependent protein-folding effects can be realized in artificial nanosystems and provides a proof of principle that nanohybrid materials decorated with structured and adjustable peptide units can be fabricated using our strategy, from which smart and responsive organic/inorganic hybrid materials capable of sensing and controlling diverse biological molecular recognition events can be developed.

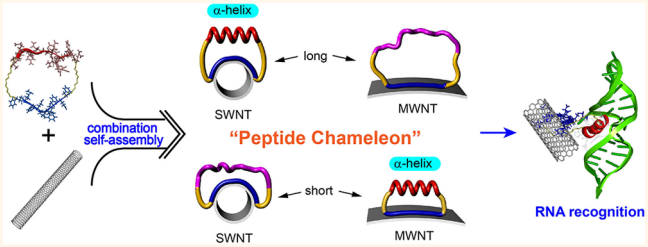

KEYWORDS: self-assembly · macrocyclic peptides · adaptable materials · carbon nanotubes · hybrid materials · α-helix

The ordering of molecules to well-defined nanocale objects by the process of self-assembly is the principle behind the formation of many natural and biological nanostructures. In many cases, nature uses the strategy to hybridize organic and inorganic molecules/materials in order to produce more sophisticated nanostructures with advanced functions.[1−5] Self-assembled peptide nanostructures (SPNs) are organic nanomaterials that have gained increased interest during recent years.[6−11] Although SPNs by themselves have great potential to be used in a wide range of applications, their functions can be diversified when the self-assembling peptides are combined with inorganic materials. For instance, self-assembly of peptides in combination with inorganic nanomaterial can provide molecular recognition function to inorganic materials. Inversely, peptide-based nanostructures can become structurally more robust and have additional physical, electrical, and photophysical properties by the hybridization. Formation of well-ordered and stable structures is important for the proper function of peptides/proteins. However, peptides self-assembled in the presence of inorganic nanostructures have not been able to attain the level of ordering and structural stability when compared to the hybrid nanostructures found in nature.

The field of peptide helix stabilization is currently an active area of research. The α-helix, which accounts for more than 30% of secondary structures in globular proteins, is responsible for mediating many biomacromolecular recognition events such as protein−protein, protein−DNA, and protein−RNA interactions.[12−14] The α-helical structures are well stabilized when they exist as a part of folded proteins; however, they typically become unstructured through a helix−coil transition when isolated from the intact protein, due to the inherent thermodynamic instability of peptides and the absence of exogenous stabilizing factors.[15] Thus, many attempts have been made to devise a strategy for stabilizing the α-helical structure of the peptide, and many stabilized α-helical peptides and peptidomimetics have been shown to be effective in modulating biomacromolecular interactions.[15−23]

Constraining the conformations of peptides that have high propensities for forming α-helices is among the most effective strategies for stabilizing α-helical structures.

* Address correspondence to yblim@yonsei.ac.kr.

Received for review April 23, 2013 and accepted July 11, 2013.

Published online July 11, 2013
10.1021/nn402025r

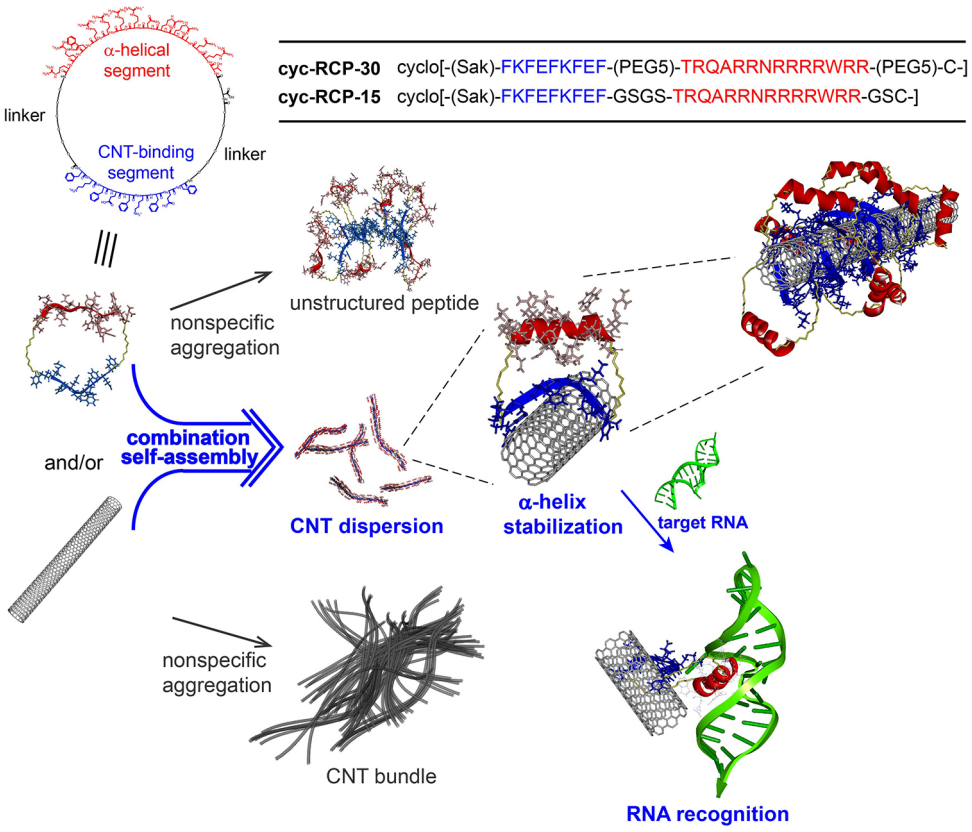

Figure 1. Pathway for the development of structured and adaptable peptide/CNT hybrid materials. Combination self-assembly between the peptide and the CNT can lead to the stabilization of the α-helix. The stabilized Rev α-helix can specifically recognize its target RRE RNA.

In these approaches, covalent linkers, which are often rigid, connect the side chains located on the same face of the helix to decrease the conformational entropy of the unfolded state.[19,24] A similar but different method of stabilizing peptide α-helices is the self-assembly approach.[25] It has been demonstrated that the self-assembly-induced transition from a flexible coil to a rigid rod in the self-assembling segment can constrain and subsequently stabilize an α-helical segment when both segments are located within the same macrocyclic scaffold.[17,26] In contrast, an α-helix could not be stabilized when a similar self-assembled peptide with a linear topology was used.[11]

Carbon nanotubes (CNTs) have many attractive physicochemical properties for use in nanobiotechnology.[27] One problem inherent to CNTs, due to their strongly hydrophobic nature, is that they are insoluble in aqueous solution and extensively bundled *via* intertube van der Waals interactions.[28] The noncovalent attachment of amphiphilic molecules on the outer surface of the CNTs can preserve the extended π networks, enhance the water solubility, individualize the CNT bundles, and specifically functionalize the CNTs. Many biomolecules, including nucleic acids, phospholipids, carbohydrates, proteins, and peptides, have been used to noncovalently functionalize CNTs.[27,29−35] By functionalizing the CNTs with proteins or peptides, organic−inorganic hybrid materials have been fabricated that can be both soft and hard and may display synergistic phenomena based on their intriguing properties.[30,35−37]

Here we present the chameleon-like behaviors of macrocyclic self-assembling peptides that can adjust and stabilize their conformation depending on the diameter/curvature of CNTs. We initially intended to develop a strategy for stabilizing the α-helical peptide structures on the surfaces of CNTs while simultaneously solubilizing the CNTs. While performing the experiment, we noticed the interesting behaviors of the designed self-assembling peptides in that they could sense the diameter/curvature of carbon nanotubes (single-walled carbon nanotubes *vs* multiwalled carbon nanotubes) and then adjusted their overall structures from disordered states to α-helices, and *vice versa*. This phenomenon is similar to the context-dependent effects in protein folding in which a single peptide unit can adopt multiple secondary structures depending on the protein tertiary environment.[38]

RESULTS AND DISCUSSION

We designed a peptide that consists of a potential α-helical segment (a peptide with a high propensity for helix formation), a CNT-binding segment, and two linker segments (Figure 1, cyc-RCP-30, *i.e.*, a cyclic Rev

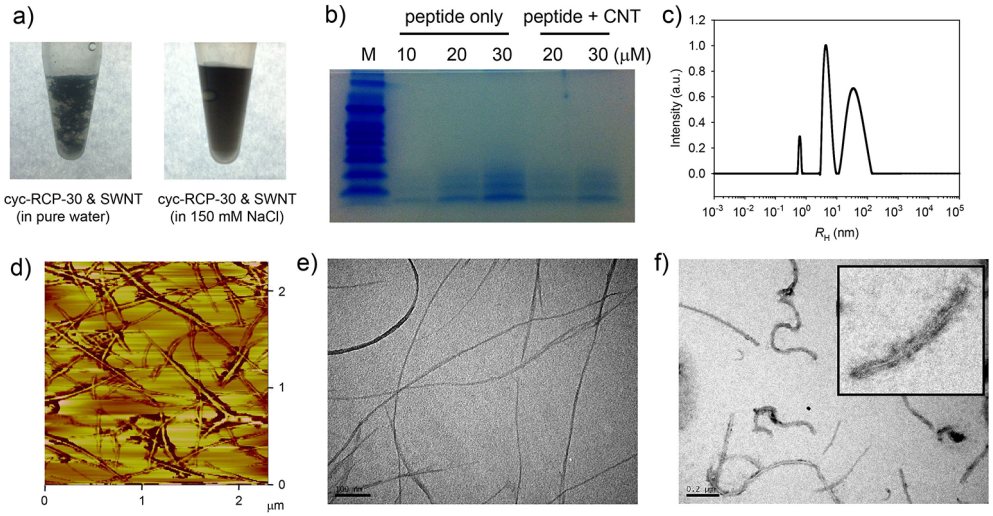

Figure 2. Formation of the cyc-RCP-30/CNT hybrids. (a) Solubilization of the SWNTs. (b) SDS-PAGE analysis to determine the amount of cyc-RCP-30 peptide bound to SWNT. Numbers indicate the concentration of cyc-RCP-30 peptide. (c) DLS analysis of the cyc-RCP-30/SWNT hybrids. (d) AFM image of the cyc-RCP-30/SWNT hybrids. TEM images of (e) the cyc-RCP-30/SWNT hybrids (bar = 100 nm) and (f) the cyc-RCP-30/MWNT hybrids (bar = 200 nm). Inset: Magnified image showing an MWNT decorated with the peptides.

CNT peptide with 30 Å linkers). The peptides were designed to be structurally cyclic, with head-to-tail cyclization. We hypothesized that the macrocyclic peptides might become highly constrained when the CNT-binding segment adsorbs onto the surface of the CNTs, which can reduce the conformational degree of freedom while simultaneously stabilizing the α-helical segment.

The potential α-helical segment was derived from the human immunodeficiency virus type-1 (HIV-1) Rev protein. The 13 kDa Rev is an RNA-binding protein that consists of 116 amino acids including an arginine-rich motif (ARM).[25,39] The Rev-ARM (approximately 14−17 amino acids) has demonstrated a high propensity for helix formation and binds its target RNA (Rev-response element, RRE) in an α-helical conformation in which the specificity of the interaction correlates well with the helicity.[12,40] The CNT-binding segment is a repeating segment of hydrophobic and positively or negatively charged amino acids (-Phe-Lys-Phe-Glu-). Such an arrangement of amino acids has been shown to promote the binding of the peptide segment at the outer surface of the CNT with relatively high ionic strength conditions.[27] Oligoethylene glycol-based hydrophilic linkers (length ~30 Å) were used to connect the helical and CNT-binding segments. The linear peptides were synthesized using a standard Fmoc solid-phase peptide synthesis (SPPS) protocol on a Rink amide MBHA resin. A head-to-tail cyclization reaction was performed, while the protected peptide remained bound to the resin to achieve a pseudo-dilution effect.[17]

We first examined whether the functionalization with cyc-RCP-30 could solubilize and debundle highly aggregated single-walled carbon nanotube (SWNT) bundles. The arc-produced SWNTs were suspended in tetrahydrofuran (THF), and 20 μg was added to a microcentrifuge tube. After evaporating the THF, an aqueous solution of the cyc-RCP-30 (40 μM, 300 μL, *i.e.*, 12 nmol of peptide) was added, and the mixture was sonicated for 30 min. The hydrophobic phenylalanine residues in the CNT-binding segment of the peptide likely interact with the SWNT, while the highly charged and hydrophilic arginine residues in the α-helical segment help disperse the peptide/SWNT hybrids in the aqueous solution. As shown in Figure 2a (left), the SWNTs were only slightly dispersed and remained highly aggregated under these conditions, suggesting that the interactions between the peptides and SWNTs are not sufficiently strong for complete solubilization of the SWNTs. However, the SWNTs became completely solubilized when the ionic strength of the solution was increased by adding sodium chloride (NaCl) or potassium fluoride (KF) to yield a physiological salt concentration of 150 mM (Figure 2a, right). The KF was used because it is typically preferred over NaCl for increasing the ionic strength during circular dichroism (CD) measurements because the chloride ion has a strong UV absorbance at low wavelengths. The strengthened hydrophobic interactions and screening of the local charges on the lysine and glutamic acid residues in the CNT-binding segment under conditions of high ionic strength are likely responsible for the enhanced peptide binding to the SWNTs, which is followed by the solubilization of the SWNTs.[27] It should be noted that the peptide molecules were completely adsorbed onto the SWNTs in this condition (*vide infra*).

Next, we quantified the maximum possible amount of peptide (cyc-RCP-30) that can be adsorbed onto the SWNT. The peptide/SWNT hybrids were first separated from the solution by centrifugation. To quantify

the amount of free peptide left in the supernatant, we performed gel electrophoresis under denaturing conditions (sodium dodecyl sulfate-polyacrylamide gel electrophoresis; SDS-PAGE) while increasing peptide concentrations (Figure 2b). Then we compared the intensity of bands of the peptide from the supernatant with that of separately loaded bands of free peptide by densitometric analysis. This analysis revealed that the binding event is almost quantitative and up to 15.6 nmol of the peptide can be adsorbed for 20 μg of the SWNTs. Considering the specific surface area of SWNTs (1315 m^2/g)[41] and the calculated surface area of the CNT-binding segment by molecular modeling (2.54×10^6 m^2/mol), the coverage of CNT surface area with the peptide is ~100%. The surface area of the CNT-binding peptide segment facing the CNT was calculated using the Corey–Pauling–Koltun space-filling model of the peptide (Accelrys Discovery Studio).

An investigation of hydrodynamic radius (R_H) of the hybrid *via* dynamic light scattering (DLS) showed the formation of a stable suspension of nano-objects with multimodal size distribution (Figure 2c). The solubilized cyc-RCP-30/SWNT hybrids were then characterized using atomic force microscopy (AFM) and transmission electron microscopy (TEM). The results revealed that most of the SWNTs were efficiently unbundled when the hybrids were prepared at high ionic strength (Figure 2d,e). Further investigation using multiwalled carbon nanotubes (MWNTs) showed that the cyc-RCP-30 can also effectively solubilize, debundle, and decorate the MWNTs under similar experimental conditions to those for SWNTs (Figure 2f).

We next used CD spectroscopy to examine the secondary structure of the cyc-RCP-30 before and after binding to the SWNTs. Before binding to the SWNTs, the cyc-RCP-30 in pure water was found to exist primarily in a random coil conformation, as indicated by a strong negative band at 198 nm (Figure 3a). Although the strong negative band was slightly red-shifted to 200 nm under the condition of high ionic strength, the peptide also existed in largely unstructured conformation (Figure 3b). These observations suggest that constraining the peptide by head-to-tail cyclization alone is insufficient to fully stabilize the α-helix because the macrocycle is large and flexible. In stark contrast, a remarkable change in the CD spectrum was observed when the peptide self-assembled in combination with the SWNTs at high ionic strength (Figure 3c). The spectrum exhibited pronounced double negative minima at 205 and 221 nm, indicating that the helical content significantly increased after the peptide/SWNT hybrid formed. This result suggests that the CNT-binding segment underwent a change from a flexible state to a rigid state upon SWNT binding.[17,26] The macrocyclic peptide then became conformationally constrained, causing the subsequent stabilization of the α-helix (Figure 1).

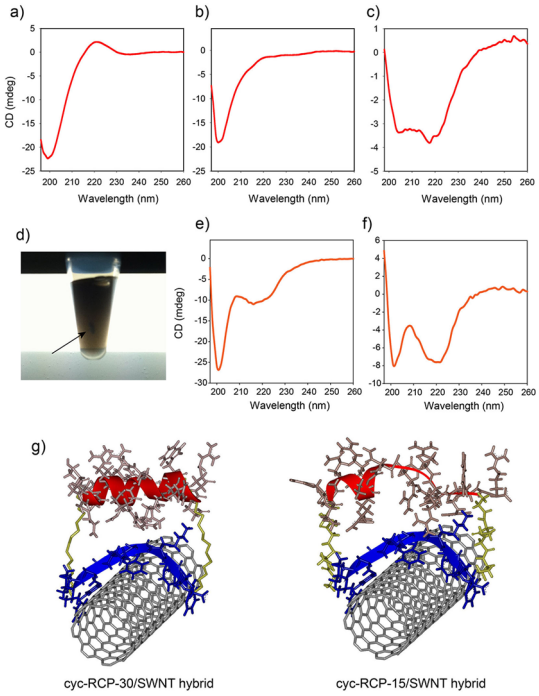

Figure 3. Combination self-assembly between the macrocyclic peptides and SWNTs. The CD spectra of cyc-RCP-30 (a) in pure water and (b) in 150 mM KF. (c) CD spectra of the cyc-RCP-30/SWNT hybrid in 150 mM KF. (d) Colloidal suspension of the cyc-RCP-15/SWNT hybrid in 150 mM KF. An arrow indicates a mark on the back of the tube to demonstrate the transparency of the suspension. The CD spectra of (e) cyc-RCP-15 and (f) cyc-RCP-15/SWNT hybrid in 150 mM KF. All CD measurements were performed at 25 °C. (g) Molecular models for the cyclic peptide/SWNT hybrids.

The diameter of the SWNTs used in this study was approximately 10–12 Å. In comparison, the fully stretched CNT-binding segment was approximately 30–35 Å in length. For this reason, the CNT-binding segment can be rolled up onto the SWNT, with a structure similar to that of DNA after SWNT binding.[42,43] This event can induce curvature in the CNT-binding segment (Figure 3g, left image). Thus, we speculated that a critical linker length could provide optimal stabilization of the α-helix. To better understand the structural basis for the CNT-binding and α-helix stabilization, we synthesized a cyclic peptide with a shorter linker length (cyc-RTC-15; linker length ~15 Å). Similar to the cyc-RCP-30 peptide, the cyc-RCP-15 existed primarily in a random coil conformation in the absence of SWNTs (Figure 3e). The cyc-RCP-15 could also efficiently solubilize the SWNTs (Figure 3d), and a large conformational change was observed in the CD profile when the cyc-RCP-15 and SWNT formed a hybrid (Figure 3f). However, the CD spectra for the cyc-RCP-15/SWNT hybrids revealed strong negative bands at 201 and 221 nm, showing the presence of a larger proportion of disordered structures than that in cyc-RCP-30/SWNT hybrids. The results indicate that the linker should be long enough to provide sufficient geometrical space for optimal α-helix stabilization; otherwise, the

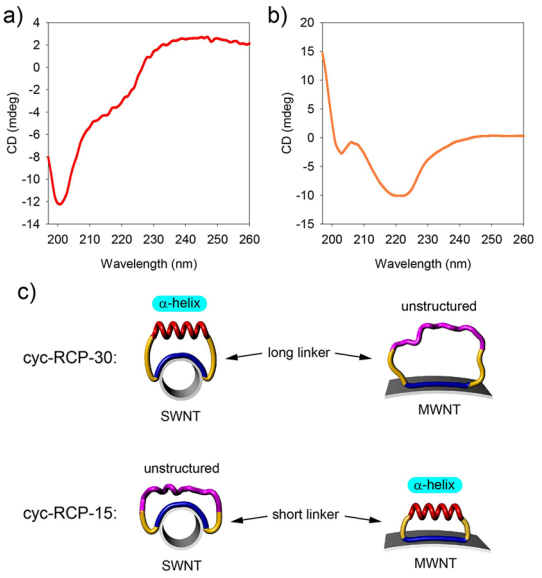

Figure 4. CNT-binding peptide chameleon changes its conformation depending on the diameter/curvature of CNTs. CD spectra of (a) cyc-RCP-30/MWNT hybrid and (b) cyc-RCP-15/MWNT hybrid in 150 mM KF. (c) Conformational change in the macrocyclic peptides depending on the diameter/curvature of CNTs. The diameters of SWNT and MWNT used in these models are 10 and 125 Å, respectively.

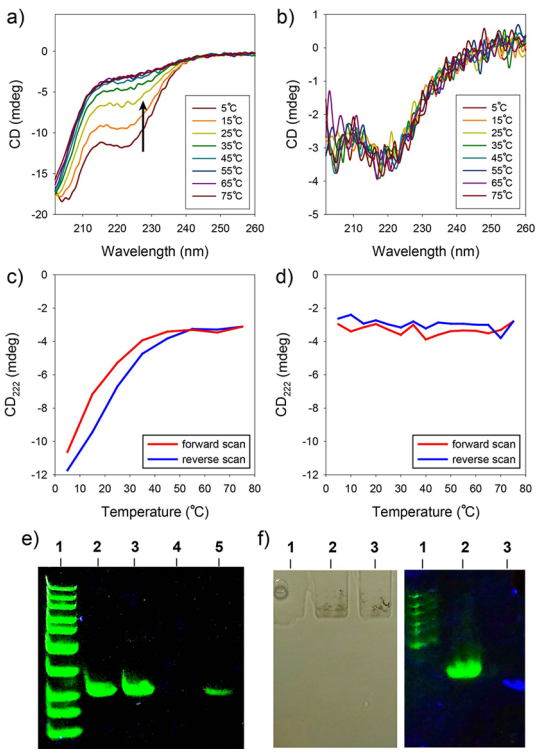

Figure 5. Thermal stability of an α-helix. (a) Temperature-dependent CD spectra and (c) changes in the CD values at 222 nm for Suc-Rev-A_4RK. (b) Temperature-dependent CD spectra and (d) changes in the CD values at 222 nm for the cyc-RCP-30/SWNT hybrid. (e and f) Electrophoretic mobility shift assay (EMSA) for RNA recognition. (e) Lane 1, DNA ladder; lane 2, wild-type RRE RNA; lane 3, mutant RRE RNA; lane 4, cyc-RCP-30/SWNT/wild-type RRE RNA mixture; lane 5, cyc-RCP-30/SWNT/mutant RRE RNA mixture. (f) Left, a bright field image; right, a fluorescence image. Lanes 1, DNA ladder; lanes 2, cyc-RCP-30/SWNT/mutant RRE RNA mixture; lanes 3, cyc-RCP-30/SWNT/wild-type RRE RNA mixture.

potential α-helical segment could be forced into excessive stretching (Figure 3g, right image).

We then investigated the secondary structure of the macrocyclic peptides after binding to MWNTs. Interestingly, there was a drastic change in the CD profile of the cyc-RCP-30 when the peptide made hybrids with the MWNTs (Figure 4a). The signature for α-helix present in the cyc-RCP-30/SWNT hybrids disappeared, and the peptide was shown to exist mostly in random coil conformation. Considering the diameter of the MWNT used (100−150 Å), the CNT-binding segment should become almost fully stretched, thus preventing the linker and potential α-helical segments from being effectively constrained for helix stabilization (Figure 4c). Conversely, the overall α-helical content of the cyc-RCP-15 increased when the peptide made hybrids with the MWNTs, as evidenced by a large increase in CD intensity at 222 nm (Figure 4b). During the combination self-assembly between the cyc-RCP-15 and the MWNTs, the limited linker length in the cyc-RCP-15 can be compensated because the CNT-binding segment would become almost fully stretched (Figure 4c). Likewise, the α-helical content of the cyc-RCP-15 also increased when the MWNTs with diameters of 60−90 Å were used (Figure S6). Therefore, the α-helix of the cyc-RCP-15 would become stabilized when the diameter of MWNTs exceeds a certain limit. Taken together, this observation demonstrates that this type of CNT-binding macrocyclic peptides can sense the diameter/curvature of CNTs and then adjust their overall structures accordingly.

Helix formation is an enthalpy-driven process in which the level of helix stabilization increases with decreasing temperature.[44] Thus, α-helices are typically destabilized as the temperature increases and *vice versa*. The linear peptide with a Rev-ARM sequence alone exhibits little helicity under ambient conditions. To cause a detectable temperature-dependent change in the helicity, the N-terminus of the Rev-ARM was succinylated, and a section of alanine and positively charged amino acids were added to the C-terminus of the Rev-ARM peptide, which has been shown to stabilize the helix macrodipole.[40,44] The modified Rev-ARM peptide (suc-Rev-A_4RK) was shown to be partially helical at low temperatures (Figure 5a). As expected, the suc-Rev-A_4RK exhibited a temperature-dependent rapid decrease in helicity (Figure 5a). The CD signal at 222 nm, a signature of an α-helix, also sharply increased, indicating the rapid destabilization of the α-helix with increasing temperature (Figure 5c). However, a temperature ramp experiment revealed that the α-helical structures in the peptide/CNT hybrids remained fully stable even when the temperature was increased to 75 °C (Figure 5b,d and Figure S8).

Many thermostable proteins exhibit a significant increase in the number of hydrophobic residues, especially

in the core of the structure or at a subunit interface.[45] Because hydrophobic effects increase with temperature, the increased hydrophobic interaction at higher temperatures is believed to be an important factor for the stabilization of thermostable proteins.[45] Moreover, the oligomerization of monomeric subunits has been shown to improve the stability of many thermophiles.[46,47] Considering these facts, strong hydrophobic and $\pi-\pi$ stacking interactions between the phenylalanine residues in the CNT-binding segment and the SWNT combined with the oligomerization of multiple peptides along the SWNT scaffold are likely responsible for the high thermostability observed in the cyc-RCP-30/SWNT hybrids.

We then tested whether the cyc-RCP-30/SWNT hybrid can differentiate between its binding partner RNA and a nonspecific one. As previously mentioned, the Rev can specifically recognize its target RRE RNA. As shown in Figure 5e and f, wild-type RRE RNA could not migrate through the gel due to the specific complex formation with the cyc-RCP-30/SWNT hybrid, whereas mutant RRE RNA could (Figures 5e,f and S3; for details, see the Supporting Information). Thus, the EMSA results revealed that the cyc-RCP-30/SWNT hybrid could indeed bind strongly to its target RRE RNA. Therefore, the helix-stabilized peptide/SWNT hybrid is functional and bioactive. This result is in agreement with the previous reports that biomolecules at the surface provide the biological identity of nanomaterials and defines the biological interactions of the nanoparticles.[48]

CONCLUSIONS

We developed a novel strategy for fabricating hybrid materials coated with multiple structured peptides, in which α-helices on the surface of a CNT are well-stabilized. Interestingly, the macrocyclic peptides could switch from disordered structures to α-helices, and *vice versa*, depending on the diameter/curvature of CNTs. In the course of the CNT adsorption and the helix stabilization, the peptide designed with cyclic topology effectively solubilized and individualized the CNTs. The α-helical structure was highly thermostable, remaining fully stable at least up to 75 °C. The stabilized Rev α-helix in the hybrid could mediate specific recognition of its cognate RNA. This study demonstrates a proof of principle that CNT-based biohybrids with stable α-helical structures can be fabricated when the as-described macrocyclic peptide strategy is applied. The biohybrids described here can become a basis of smart and responsive materials that can sense and control diverse biological events.

MATERIALS AND METHODS

Materials. Fmoc-amino acids and the oligoethylene glycol-based linker Fmoc-21-amino-4,7,10,13,16,19-hexaoxaheneicosanoic acid (Fmoc-NH-(PEG)5-COOH, 22 atoms) were purchased from Novabiochem. Carbon nanotubes were obtained from Hanhwa Nanotech. RNA oligos were purchased from Integrated DNA Technologies.

Peptide Synthesis and Macrocyclization Reaction. The peptide was synthesized on Rink amide MBHA resin LL (Novabiochem) using standard Fmoc protocols on a Tribute peptide synthesizer (Protein Technologies, Inc.). Standard amino acid protecting groups were employed except cysteine, in which an acid-labile methoxytrityl (Mmt) group was used. For cyclization, the peptide-attached resin (20 μmol in terms of N-terminal amine groups) was swollen in *N*-methyl-2-pyrrolidone (NMP) for 30 min. Then, bromoacetic acid was first coupled to the N-terminal part of the resin-bound peptide. Before addition to the resin, a mixture of bromoacetic acid (28 mg, 200 μmol) and *N,N′*-diisopropylcarbodiimide (15.5 μL, 100 μmol) in NMP was incubated for 10 min for carboxyl activation. Following addition of the mixture to the resin, the reaction was continued for 1 h with shaking at room temperature, in a 6 mL polypropylene tube with a frit (Restek). The resin was then washed successively with NMP and dichloromethane (DCM). For orthogonal deprotection of the Mmt group from the cysteine, the resin was treated with 1% trifluoroacetic acid (TFA) in DCM several times (1 min × ~7). Intramolecular cyclization reaction was performed in 3 mL of 1% *N,N*-diisopropylethylamine in NMP overnight with shaking at room temperature. The resin was then successively washed with NMP, DMF, and THF and dried under reduced pressure. For cleavage and final deprotection, the resin was treated with cleavage cocktail (TFA:1,2-ethanedithiol:thioanisole; 95:2.5:2.5) for 3 h and was triturated with *tert*-butyl methyl ether. The peptides were purified by reverse-phase HPLC (water/acetonitrile with 0.1% TFA). The molecular weight was confirmed by MALDI-TOF mass spectrometry. The purity of the peptides was >95% as determined by analytical HPLC. The peptide concentration was determined spectrophotometrically in water/acetonitrile (1:1) using a molar extinction coefficient of tryptophan (5500 M^{-1} cm^{-1}) at 280 nm.

Quantification of the Amount of Adsorbed Peptide in Peptide/CNT Hybrids. The arc-produced SWNTs were suspended in THF at 250 μg/mL, and 20 μL (5 μg) was added to a microcentrifuge tube. THF was evaporated using a centrifugal evaporator. After evaporating the THF, various concentrations of the cyc-RCP-30 in water (300 μL) were added, and the mixture was sonicated for 30 min. Then NaCl was added to a final concentration of 150 mM, and the solution was further sonicated. The suspension was centrifuged at 16110*g* at 4 °C for 1 h, and the pellet that contains the peptide/SWNT hybrids was discarded. The supernatants (10 μL) were then subjected to 10% SDS-PAGE analysis in Tris-tricine buffer systems at 100 V. The free peptide at various concentrations was simultaneously electrophoresed as a reference for quantification. The gel was stained with Brilliant Blue G (Sigma-Aldrich), and the densitometric analysis of the peptide band intensity was performed with Adobe Photoshop software.

Electrophoretic Mobility Shift Assay. Wild-type RRE IIB RNA sequence: 5′-GAC CUG GUA UGG GCG CAG CGC AAG CUG ACG GUA CAG GCC AGG UC-3′. Mutant RRE IIB RNA sequence: 5′-GAC CUG GUA UCG GCG CAG CGC AAG CUG ACG GUA GAG GCC AGG UC-3′.

The SWNTs were suspended in THF, and 20 μg was added to a microcentrifuge tube. After evaporating the THF, an aqueous solution of the cyc-RCP-30 (40 μM, 300 μL) was added, and the mixture was sonicated for 30 min. For the cyc-RCP-30/SWNT hybrid formation, NaCl was added to a final concentration of 150 mM, and the solution was sonicated. The suspension was centrifuged at 16110*g* for 10 min, and the supernatant was removed. The pellet (the cyc-RCP-30/SWNT hybrid) was resuspended with 50 μL of 1 μM RNA solution in 150 mM NaCl. The ternary complex (the peptide/SWNT/RNA) formed a stable suspension. The complex was incubated at room temperature for 30 min and then at 4 °C for 30 min. Ten microliters of the ternary complex was electrophoresed on a nondenaturing polyacrylamide gel (10% polyacrylamide, 0.5 × TBE) at 200 V, 4 °C. RNA was visualized with a SYBR Green II RNA gel stain reagent (Invitrogen).

Conflict of Interest: The authors declare no competing financial interest.

Supporting Information Available: Peptide chemical structures, MALDI-TOF MS spectra, additional CD data, EMSA results, and details of the experimental procedures. This material is available free of charge *via* the Internet at http://pubs.acs.org.

Acknowledgment. This work was supported by grants from the National Research Foundation (NRF) of Korea (2012R1A1A2006453, 2009-0092971, 2013M2B2A4041202) and from the Seoul R&BD program (ST110029).

REFERENCES AND NOTES

1. Ruiz-Hitzky, E.; Darder, M.; Aranda, P.; Ariga, K. Advances in Biomimetic and Nanostructured Biohybrid Materials. *Adv. Mater.* **2010**, *22*, 323–336.
2. Ge, J.; Lei, J.; Zare, R. N. Protein-Inorganic Hybrid Nanoflowers. *Nat. Nanotechnol.* **2012**, *7*, 428–432.
3. Kotov, N. A. Chemistry. Inorganic Nanoparticles as Protein Mimics. *Science* **2010**, *330*, 188–189.
4. Descalzo, A. B.; Martinez-Manez, R.; Sancenon, F.; Hoffmann, K.; Rurack, K. The Supramolecular Chemistry of Organic-Inorganic Hybrid Materials. *Angew. Chem., Int. Ed.* **2006**, *45*, 5924–5948.
5. Hoffmann, F.; Cornelius, M.; Morell, J.; Froba, M. Silica-Based Mesoporous Organic-Inorganic Hybrid Materials. *Angew. Chem., Int. Ed.* **2006**, *45*, 3216–3251.
6. Gazit, E. Self-Assembled Peptide Nanostructures: The Design of Molecular Building Blocks and Their Technological Utilization. *Chem. Soc. Rev.* **2007**, *36*, 1263–1269.
7. Lim, Y. B.; Moon, K. S.; Lee, M. Recent Advances in Functional Supramolecular Nanostructures Assembled from Bioactive Building Blocks. *Chem. Soc. Rev.* **2009**, *38*, 925–934.
8. Zelzer, M.; Ulijn, R. V. Next-Generation Peptide Nanomaterials: Molecular Networks, Interfaces and Supramolecular Functionality. *Chem. Soc. Rev.* **2010**, *39*, 3351–3357.
9. Konig, H. M.; Kilbinger, A. F. Learning from Nature: β-Sheet-Mimicking Copolymers Get Organized. *Angew. Chem., Int. Ed.* **2007**, *46*, 8334–8340.
10. Hamley, I. W. Peptide Fibrillization. *Angew. Chem., Int. Ed.* **2007**, *46*, 8128–8147.
11. Han, S.; Kim, D.; Han, S. H.; Kim, N. H.; Kim, S. H.; Lim, Y. B. Structural and Conformational Dynamics of Self-Assembling Bioactive β-Sheet Peptide Nanostructures Decorated with Multivalent RNA-Binding Peptides. *J. Am. Chem. Soc.* **2012**, *134*, 16047–16053.
12. Battiste, J. L.; Mao, H.; Rao, N. S.; Tan, R.; Muhandiram, D. R.; Kay, L. E.; Frankel, A. D.; Williamson, J. R. α Helix-RNA Major Groove Recognition in an HIV-1 Rev Peptide-RRE RNA Complex. *Science* **1996**, *273*, 1547–1551.
13. Kussie, P. H.; Gorina, S.; Marechal, V.; Elenbaas, B.; Moreau, J.; Levine, A. J.; Pavletich, N. P. Structure of the MDM2 Oncoprotein Bound to the p53 Tumor Suppressor Transactivation Domain. *Science* **1996**, *274*, 948–953.
14. Pabo, C. O.; Peisach, E.; Grant, R. A. Design and Selection of Novel Cys_2His_2 Zinc Finger Proteins. *Annu. Rev. Biochem.* **2001**, *70*, 313–340.
15. Liu, J.; Wang, D.; Zheng, Q.; Lu, M.; Arora, P. S. Atomic Structure of a Short α-Helix Stabilized by a Main Chain Hydrogen-Bond Surrogate. *J. Am. Chem. Soc.* **2008**, *130*, 4334–4337.
16. Bodkin, M. J.; Goodfellow, J. M. Competing Interactions Contributing to α-Helical Stability in Aqueous Solution. *Protein Sci.* **1995**, *4*, 603–612.
17. Lim, Y. B.; Moon, K. S.; Lee, M. Stabilization of an α Helix by β-Sheet-Mediated Self-Assembly of a Macrocyclic Peptide. *Angew. Chem., Int. Ed.* **2009**, *48*, 1601–1605.
18. Verma, A.; Nakade, H.; Simard, J. M.; Rotello, V. M. Recognition and Stabilization of Peptide α-Helices Using Templatable Nanoparticle Receptors. *J. Am. Chem. Soc.* **2004**, *126*, 10806–10807.
19. Zhang, F. Z.; Sadovski, O.; Xin, S. J.; Woolley, G. A. Stabilization of Folded Peptide and Protein Structures *via* Distance Matching with a Long, Rigid Cross-Linker. *J. Am. Chem. Soc.* **2007**, *129*, 14154–14155.
20. Henchey, L. K.; Jochim, A. L.; Arora, P. S. Contemporary Strategies for the Stabilization of Peptides in the α-Helical Conformation. *Curr. Opin. Chem. Biol.* **2008**, *12*, 692–697.
21. Bernal, F.; Tyler, A. F.; Korsmeyer, S. J.; Walensky, L. D.; Verdine, G. L. Reactivation of the p53 Tumor Suppressor Pathway by a Stapled p53 Peptide. *J. Am. Chem. Soc.* **2007**, *129*, 2456–2457.
22. Edwards, T. A.; Wilson, A. J. Helix-Mediated Protein-Protein Interactions as Targets for Intervention Using Foldamers. *Amino Acids* **2011**, *41*, 743–754.
23. Saraogi, I.; Hamilton, A. D. α-Helix Mimetics as Inhibitors of Protein-Protein Interactions. *Biochem. Soc. Trans.* **2008**, *36*, 1414–1417.
24. Fujimoto, K.; Oimoto, N.; Katsuno, K.; Inouye, M. Effective Stabilisation of α-Helical Structures in Short Peptides with Acetylenic Cross-Linking Agents. *Chem. Commun.* **2004**, 1280–1281.
25. Han, S. H.; Lee, M. K.; Lim, Y. B. Bioinspired Self-Assembled Peptide Nanofibers with Thermostable Multivalent α-Helices. *Biomacromolecules* **2013**, *14*, 1594–1599.
26. Choi, S. J.; Jeong, W. J.; Kim, T. H.; Lim, Y. B. Controlled Self-Assembly of α-Helix-Decorated Peptide Nanostructures. *Soft Matter* **2011**, *7*, 1675–1677.
27. Jeong, W. J.; Lim, Y. B. Combination Self-Assembly of β-Sheet Peptides and Carbon Nanotubes: Functionalizing Carbon Nanotubes with Bioactive β-Sheet Block Copolypeptides. *Macromol. Biosci.* **2012**, *12*, 49–54.
28. Thess, A.; Lee, R.; Nikolaev, P.; Dai, H.; Petit, P.; Robert, J.; Xu, C.; Lee, Y. H.; Kim, S. G.; Rinzler, A. G.; *et al*. Crystalline Ropes of Metallic Carbon Nanotubes. *Science* **1996**, *273*, 483–487.
29. Katz, E.; Willner, I. Biomolecule-Functionalized Carbon Nanotubes: Applications in Nanobioelectronics. *ChemPhysChem* **2004**, *5*, 1085–1104.
30. Kim, J. H.; Ahn, J. H.; Barone, P. W.; Jin, H.; Zhang, J. Q.; Heller, D. A.; Strano, M. S. A Luciferase/Single-Walled Carbon Nanotube Conjugate for Near-Infrared Fluorescent Detection of Cellular ATP. *Angew. Chem., Int. Ed.* **2010**, *49*, 1456–1459.
31. Tu, X. M.; Manohar, S.; Jagota, A.; Zheng, M. DNA Sequence Motifs for Structure-Specific Recognition and Separation of Carbon Nanotubes. *Nature* **2009**, *460*, 250–253.
32. Wu, P.; Chen, X.; Hu, N.; Tam, U. C.; Blixt, O.; Zettl, A.; Bertozzi, C. R. Biocompatible Carbon Nanotubes Generated by Functionalization with Glycodendrimers. *Angew. Chem., Int. Ed.* **2008**, *47*, 5022–5025.
33. Wu, Y.; Hudson, J. S.; Lu, Q.; Moore, J. M.; Mount, A. S.; Rao, A. M.; Alexov, E.; Ke, P. C. Coating Single-Walled Carbon Nanotubes with Phospholipids. *J. Phys. Chem. B* **2006**, *110*, 2475–2478.
34. Dieckmann, G. R.; Dalton, A. B.; Johnson, P. A.; Razal, J.; Chen, J.; Giordano, G. M.; Munoz, E.; Musselman, I. H.; Baughman, R. H.; Draper, R. K. Controlled Assembly of Carbon Nanotubes by Designed Amphiphilic Peptide Helices. *J. Am. Chem. Soc.* **2003**, *125*, 1770–1777.
35. Grigoryan, G.; Kim, Y. H.; Acharya, R.; Axelrod, K.; Jain, R. M.; Willis, L.; Drndic, M.; Kikkawa, J. M.; DeGrado, W. F. Computational Design of Virus-Like Protein Assemblies on Carbon Nanotube Surfaces. *Science* **2011**, *332*, 1071–1076.
36. Chen, C. L.; Rosi, N. L. Peptide-Based Methods for the Preparation of Nanostructured Inorganic Materials. *Angew. Chem., Int. Ed.* **2010**, *49*, 1924–1942.
37. Lee, Y.; Geckeler, K. E. Carbon Nanotubes in the Biological Interphase: The Relevance of Noncovalence. *Adv. Mater.* **2010**, *22*, 4076–4083.
38. Minor, D. L., Jr.; Kim, P. S. Context-Dependent Secondary Structure Formation of a Designed Protein Sequence. *Nature* **1996**, *380*, 730–734.
39. Pollard, V. W.; Malim, M. H. The HIV-1 Rev Protein. *Annu. Rev. Microbiol.* **1998**, *52*, 491–532.
40. Tan, R.; Chen, L.; Buettner, J. A.; Hudson, D.; Frankel, A. D. RNA Recognition by an Isolated α Helix. *Cell* **1993**, *73*, 1031–1040.

41. Peigney, A.; Laurent, C.; Flahaut, E.; Bacsa, R. R.; Rousset, A. Specific Surface Area of Carbon Nanotubes and Bundles of Carbon Nanotubes. *Carbon* **2001**, *39*, 507–514.
42. Tu, X.; Manohar, S.; Jagota, A.; Zheng, M. DNA Sequence Motifs for Structure-Specific Recognition and Separation of Carbon Nanotubes. *Nature* **2009**, *460*, 250–253.
43. Heller, D. A.; Jeng, E. S.; Yeung, T. K.; Martinez, B. M.; Moll, A. E.; Gastala, J. B.; Strano, M. S. Optical Detection of DNA Conformational Polymorphism on Single-Walled Carbon Nanotubes. *Science* **2006**, *311*, 508–511.
44. Marqusee, S.; Robbins, V. H.; Baldwin, R. L. Unusually Stable Helix Formation in Short Alanine-Based Peptides. *Proc. Natl. Acad. Sci. U.S.A.* **1989**, *86*, 5286–5290.
45. Petsko, G. A. Structural Basis of Thermostability in Hyperthermophilic Proteins, or "There's More Than One Way to Skin a Cat". *Methods Enzymol.* **2001**, *334*, 469–478.
46. Flores, H.; Ellington, A. D. Increasing the Thermal Stability of an Oligomeric Protein, β-Glucuronidase. *J. Mol. Biol.* **2002**, *315*, 325–337.
47. Choi, S. J.; Jeong, W. J.; Kang, S. K.; Lee, M.; Kim, E.; Ryu du, Y.; Lim, Y. B. Differential Self-Assembly Behaviors of Cyclic and Linear Peptides. *Biomacromolecules* **2012**, *13*, 1991–1995.
48. Monopoli, M. P.; Aberg, C.; Salvati, A.; Dawson, K. A. Biomolecular Coronas Provide the Biological Identity of Nanosized Materials. *Nat. Nanotechnol.* **2012**, *7*, 779–786.